# Impacts of climate change on hydrology, water quality and crop productivity in the Ohio-Tennessee River Basin


Yiannis Panagopoulos[1*], Philip W. Gassman[1], Raymond W. Arritt[2], Daryl E. Herzmann[2], Todd D. Campbell[1], Adriana Valcu[1], Manoj K. Jha[3], Catherine L. Kling[1], Raghavan Srinivasan[4], Michael White[5], Jeffrey G. Arnold[5]

(1. *Center for Agricultural and Rural Development* (*CARD*), *Iowa State University, Ames, IA 50011-1070, USA*;
2. *Department of Agronomy, 2104 Agronomy Hall, Iowa State University, Ames IA 50011-1010, USA*;
3. *Department of Civil, Architectural and Environmental Engineering, 456 McNair Hall, North Carolina A&T State University, Greensboro, NC 27411, USA*;
4. *Departments of Ecosystem Sciences and Management and Biological and Agricultural Engineering, 1500 Research Parkway, Suite B223, 220 TAMU, Texas A&M University, College Station, TX 77843-2120, USA*;
5. *Grassland Soil and Water Research Laboratory, U.S. Department of Agriculture-Agricultural Research Service, 808 East Blackland Road, Temple, TX 76502, USA*)

**Abstract:** Nonpoint source pollution from agriculture is the main source of nitrogen and phosphorus in the stream systems of the Corn Belt region in the Midwestern US. The eastern part of this region is comprised of the Ohio-Tennessee River Basin (OTRB), which is considered a key contributing area for water pollution and the Northern Gulf of Mexico hypoxic zone. A point of crucial importance in this basin is therefore how intensive corn-based cropping systems for food and fuel production can be sustainable and coexist with a healthy water environment, not only under existing climate but also under climate change conditions in the future. To address this issue, a OTRB integrated modeling system has been built with a greatly refined 12-digit subbasin structure based on the Soil and Water Assessment Tool (SWAT) water quality model, which is capable of estimating landscape and in-stream water and pollutant yields in response to a wide array of alternative cropping and/or management strategies and climatic conditions. The effects of three agricultural management scenarios on crop production and pollutant loads exported from the crop land of the OTRB to streams and rivers were evaluated: (1) expansion of continuous corn across the entire basin, (2) adoption of no-till on all corn and soybean fields in the region, (3) implementation of a winter cover crop within the baseline rotations. The effects of each management scenario were evaluated both for current climate and projected mid-century (2046-2065) climates from seven global circulation models (GCMs). In both present and future climates each management scenario resulted in reduced erosion and nutrient loadings to surface water bodies compared to the baseline agricultural management, with cover crops causing the highest water pollution reduction. Corn and soybean yields in the region were negligibly influenced from the agricultural management scenarios. On the other hand, both water quality and crop yield numbers under climate change deviated considerably for all seven GCMs compared to the baseline climate. Future climates from all GCMs led to decreased corn and soybean yields by up to 20% on a mean annual basis, while water quality alterations were either positive or negative depending on the GCM. The study highlights the loss of productivity in the eastern Corn Belt under climate change, the need to consider a range of GCMs when assessing impacts of climate change, and the value of SWAT as a tool to analyze the effects of climate change on parameters of interest at the basin scale.

**Keywords:** agricultural management scenarios, corn-based systems, global circulation models, hydrology, water quality, crop yields, SWAT, Ohio-Tennessee River Basin
**DOI:** 10.3965/j.ijabe.20150803.1497 Online first on [2015-03-19]

**Citation:** Panagopoulos Y, Gassman P W, Arritt R W, Herzmann D E, Campbell T D, Valcu A, et al. Impacts of climate change on hydrology, water quality and crop productivity in the Ohio-Tennessee River Basin. Int J Agric & Biol Eng, 2015; 8(3): 36－53.

## 1 Introduction

Over-enrichment of nutrients constitutes a major problem in many streams and rivers in the USA. In addition to local effects, transport of these nutrients contributes to environmental problems such as eutrophication in downstream lakes, bays and estuaries, and is primarily responsible for hypoxia in the Gulf of Mexico[1]. The Mississippi River/Gulf of Mexico Watershed Nutrient Task Force[2] established a goal to reduce the size of the hypoxic zone in the Gulf of Mexico to 5 000 km$^2$. This will require substantial reductions in nutrient loadings from the Misssissippi/Atchafalaya River basin (MARB) including the intensively cultivated eastern part, the Ohio-Tennessee River Basin (OTRB), which forms the eastern part of the 'Corn Belt' region of the U.S. Within this large area, trade-offs between the interdependent goals of sustainable biofuel production, food production and water resources have significant implications for commodity groups, individual producers and other stakeholders in the region.

Within this context, physically-based hydrological models can be used to evaluate socio-economic and environmental impacts of agricultural management scenarios. However, in order to reliably address what-if scenarios for future agriculture, the impacts of future climate change should also be accounted for. The Soil and Water Assessment Tool (SWAT) water quality model[3,4] has proven to be an effective tool worldwide for evaluating agricultural management practices for complex landscapes and varying climate regimes including the impacts of future climate projections on watershed hydrology and water quality as documented in several previous reviews[5-8]. Previous analyses of the OTRB with SWAT have been limited to a hydrologic calibration/validation methodology and the effects of cropland conservation practices on water quality[9-11]. Additional testing and/or assessments of cropland conservation impacts on nonpoint source pollution has also been simulated for the OTRB as part of overall SWAT Corn Belt or MARB modeling systems[12-17]. However, none of these studies investigated the impact of projected climate change on the efficiency or environmental consequences of alternative management scenarios.

We investigate here the impacts of climate projections from seven coupled atmosphere-ocean general circulation models (GCMs) for both baseline land use versus alternative cropping/management practices relevant to corn-based production systems. The study was performed within the context of the Climate and Corn-based Cropping Systems CAP (CSCAP) transdisciplinary project initiated by the U.S. Department of Agriculture[18]. The analysis was performed with a greatly refined SWAT subbasin delineation approach which allows for improved linkages to climate data, due to the structure of SWAT which requires climate data to be input to a given subbasin from the closest climate station. This refined subbasin structure allows input of downscaled, bias-corrected GCM projections across a dense grid overlaid on the OTRB study region. Thus, the specific objectives of the study are to describe the enhanced OTRB modeling system and to describe the impacts of measured baseline climate and projections

**Received date:** 2014-10-14 **Accepted date:** 2015-03-15

**Biographies: Philip W Gassman**, Environmental Scientist; Research interests: water quality and environmental modeling. Email: pwgassma@iastate.edu. **Raymond W Arritt**, Professor; Research interests: climate change and GCM models. Email: rwarritt@bruce.agron.iastate.edu. **Daryl E Herzmann**, Research Associate; Research interests: real time weather data systems, agricultural meteorology. Email: akrherz@iastate.edu. **Todd D Campbell**, Computer programmer; Research interests: databases, physical models. Email: tdc@iastate.edu. **Adriana Valcu**, Postdoctoral Research Associate; Research interests: economic and environmental impacts of agricultural practices. Email: amvalcu@iastate.edu. **Manoj K Jha**, Assistant Professor; Research interests: hydrology, water resources management. Email: mkjha@ncat.edu. **Catherine L Kling**, Distinguished Professor; Research interests: economic and environmental impacts of agricultural practices. Email: ckling@iastate.edu. **Raghavan Srinivasan**, PhD, Research interests: hydrology, watershed management, GIS. Email: r-srinivasan@tamu.edu. **Michael White**, Agricultural Engineer, Research interests: Agriculture, Hydrology. Email: mike.white@ars.usda.gov. **Jeffrey G Arnold**, Agricultural Engineer, Research interests: Agriculture, Hydrology. Email: jeff.arnold@ars.usda.gov.

***Corresponding author: Yiannis Panagopoulos**, Research Associate; Research Interests: Hydrology, Modeling, Water Resources Management. Center for Agricultural and Rural Development (CARD), Iowa State University, Ames, IA 50011-1070, USA. Email: ypanag@iastate.edu, Tel: +1-515-294-1620.

from seven GCMs for both baseline land use and three alternative land use scenarios: (1) conversion of all cropland to a continuous corn (C-C) rotation, (2) adoption of no-tillage (NT) on all cropland areas, and (3) the adoption of a winter cover crop (rye) within rotations of corn and soybean.

## 2 Materials and methods

### 2.1 Watershed Description

The OTRB covers about 528 000 km$^2$ across portions of seven states and consists of two Major Water Resource Regions (MWRRs): the Ohio River basin and the Tennessee River basin (Figure 1). These two major river systems are classified as 2-digit river basins (Ohio = 05; Tennessee = 06) within the standard U.S. federal agency watershed classification method[19] and are two of the six MWRRs that comprise the overall MARB (Figure 1). The OTRB further consists of 152 8-digit subbasins and 6 350 12-digit subbasins (Figure 2) which are additional delineations within the U.S. federal agency watershed classification method[19]. The use of 12-digit subbasins, which average roughly about 85 km$^2$ in area, provides the opportunity to more directly and accurately capture meteorological inputs from the thousands of available climate stations in the basin, which could not be fully utilized in the model with the coarser 8-digit delineation (each 8-digit watershed consists of about 40 to 45 12-digit watersheds; e.g., see Figure 2). The Ohio River starts in Pennsylvania and ends in Illinois, where it flows into the Mississippi River near the city of Metropolis (Figure 3). The Tennessee River joins the Ohio River at Paducah, Kentucky just upstream of the confluence of the Ohio and Mississippi rivers (Figure 3). The OTRB receives a high amount of annual rainfall, averaging nearly 1 200 mm/a (a denotes annual or year) over the last 40 years. The dominant land uses in the basin are forest (50%), cropland (20%) and permanent pasture/hay (15%). Corn, soybean and wheat are the major crops grown[10]. The OTRB is characterized by steep slopes, especially across much of the forested Tennessee basin. The mean annual flow is 8 400 m$^3$/s at Metropolis (Figure 3). The entire basin contributes 0.5 Gt of nitrogen (N) to the downstream Mississippi river on a mean annual basis, with about 65% of this load occurring as nitrate-nitrogen ($NO_3$-N). Phosphorus (P) loads have been measured at the most downstream USGS station equal to 48 000 t/a[20].

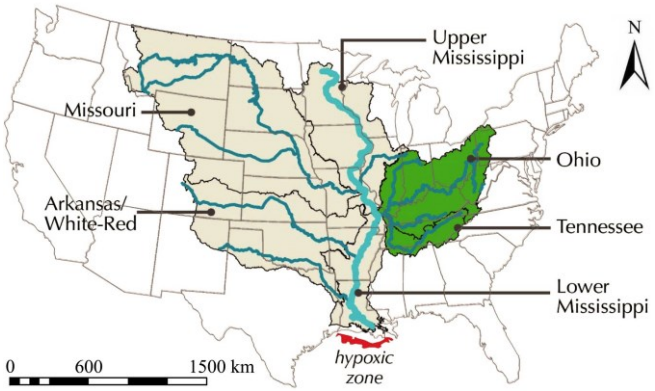


Figure 1 Location of the Ohio-Tennessee River Basin (OTRB) relative to the four other major water resource regions (MWRRs) within the overall Misissippi-Atchfalaya River Basin (MARB)

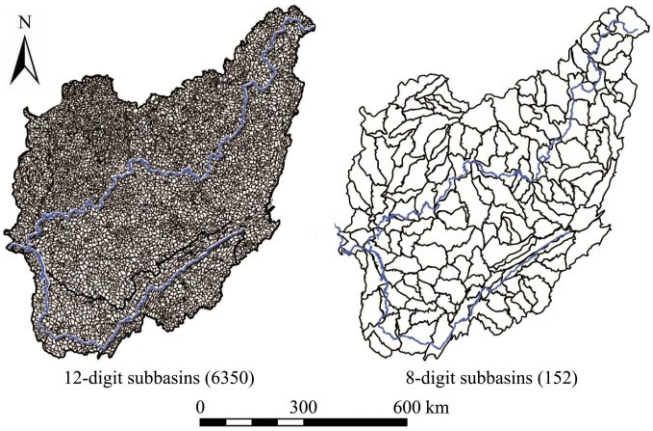


Figure 2 Comparison of the 12-digit subbasins versus 8-digit watershed delineation schemes for the Ohio-Tennessee River Basin (OTRB)

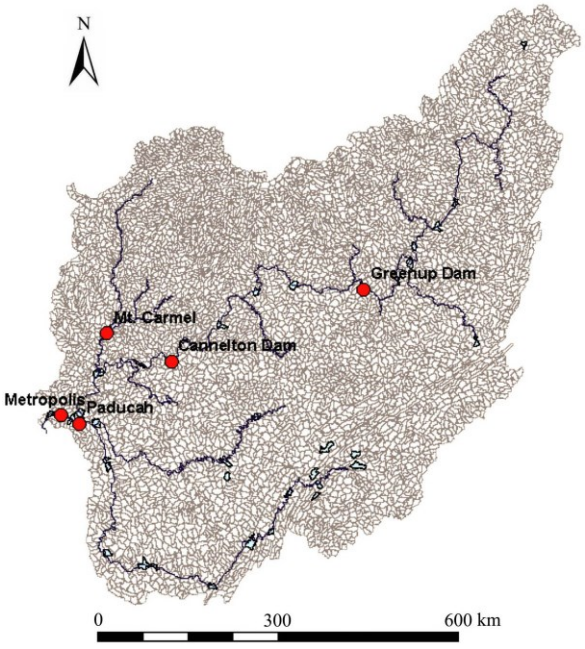


Figure 3 The OTRB delineation using 12-digit subbasins and the calibration points along the Ohio River and its tributaries

### 2.2 SWAT model description

SWAT was developed by the U.S. Department of Agriculture in collaboration with Texas A&M University[4] and is continuously upgraded with improved versions and interfaces. A recent release of SWAT version 2012[21] (SWAT2012; Release 615) in combination with the ArcGIS (version 10.1) SWAT (ArcSWAT) interface (SWAT 2013) were used in this study[22]. In SWAT, a basin is typically delineated into subbasins and subsequently into Hydrologic Response Units (HRUs), which represent homogeneous combinations of land use, soil types and slope classes in each subbasin (but are not spatially identified within a given subbasin). However, a "dominant HRU approach" can also be used in which no further delineation of subbasins occurs; i.e., a given subbasin is synonymous with a single HRU (which was the method used in this study). The physical processes associated with water and sediment movement, crops growth and nutrient cycling are modelled at the HRU scale; runoff and pollutants exported from the different HRUs are aggregated at the subbasin level and routed downstream. Simulation of the hydrology is separated into the land and routing phases of the hydrological cycle. Sediment yields generated from water erosion are estimated with the Modified Universal Soil Loss Equation (MUSLE)[23]. SWAT simulates both N and P cycling, which are influenced by specified management practices. Both N and P are divided in the soil into two parts, each associated with organic and inorganic N and P transport and transformations. Agricultural management practices can be simulated with specific dates and by explicitly defining the appropriate management parameters for each HRU. In-field conservation practices such as contour farming, strip-cropping, terraces and residue management are simulated with changes to model parameters that represent cultivation patterns[24]. A complete description of all processes simulated in the model and associated required input data are provided in the SWAT theoretical documentation[25] and users manual[21], respectively.

### 2.3 The SWAT OTRB parameterization

Key data layers that were incorporated for building the OTRB SWAT model included climate, soil, land use and topographic and management data sources. A brief overview of the data sources and modeling assumptions used for the OTRB simulations are provided here. More detailed descriptions of the modeling inputs are presented in a previous study[12].

Topography was represented by a 30 m (98.43 ft) digital elevation model[26] which was used in ArcSWAT to calculate landscape parameters such as slope and slope length. As previously noted, a greatly refined delineation scheme has been incorporated into the current model, which consists of using subbasin boundaries that are coincident with the USGS 12-digit watersheds instead of the coarser 8-digit basins which have been used in previous SWAT studies. The average area of an OTRB 12-digit basin is typically 8 300 ha versus nearly 350 000 ha for an 8-digit basin (Figure 2). Historic daily precipitation, and maximum and minimum temperatures were obtained from the National Climatic Data Center[27] and were input to the model from a total of more than 1 000 climate stations across the study region. Wind speed, relative humidity and solar radiation data, required for the estimation of potential evapotranspiration using the Penman-Monteith method[21], which was used in this study, were generated internally in SWAT using the model's weather generator.

The landuse layer of the OTRB model was created by using the USDA-NASS Cropland Data Layer (CDL) datasets[28] in combination with the 2001 National Land Cover Data[29]. This approach included the overlay of three years of CDL datasets in order to create crop rotations used in the region, similar to the approach reported in previous research for the Upper Mississippi River Basin[30]. This process resulted in dominant two-year rotations of corn and soybean (C-S) for the cropland portion of the region with a smaller fraction managed with a continuous corn (C-C) rotation. Soil characteristics were represented by the USDA 1: 250 000 STATSGO soil data[31]. The spatial resolution of these data was rather coarse with approximately 1 000 soil types lying within the OTRB. Thus, we overlaid land use and soils on each of the 6 350 subbasins in ArcSWAT and selected the dominant land use type and soil

occupying each subbasin. Therefore, the number of HRUs in this study was equal to the number of subbasins; i.e., one 12-digit subbasin equals one HRU. This approach resulted in a slight (~5%) increase of the total cropland area compared to the original land use map. A slight increase in forest also occurred, while other land cover types were reduced accordingly to maintain the sum of all land types equal to the total area of the basin. Minor rotations such as corn-corn-soybean or corn-soybean-wheat were eliminated in this process; these comprised less than 5% of the cropland area in any of the 12-digit subbasins. The OTRB cropland covered over 100 000 $km^2$ and was mainly concentrated in Illinois, Indiana and western Ohio.

Estimates of possible locations where subsurface tiles are used to drain soils, a key conduit of nitrate to surface waters, were based on areal county-level estimates[32]. Estimates at the county level were first aggregated at the 8-digit level with the use of GIS applications in order to have the same spatial reference with available fertilizer and tillage data. Tile drains were first assigned to the agricultural subbasins (12-digit basins) within each 8-digit basin with slopes lower than 2% and with poorly drained soils (hydrologic groups D or C), and subsequently to low-slope, hydrologic group B soils if needed. All tile drains were simulated with the following assumptions: depth of 1 200 mm (3.94 ft), time to drain a soil to field capacity (24 h), and time required to release water from a drain tile to a stream reach (72 h), which are the SWAT DDRAIN, TDRAIN, and GDRAIN input parameters[21], respectively.

Spatial representation of various tillage types (conventional, reduced, mulch and no-till) were incorporated in the modeling system using estimates of the distributions of different tillage types at the 8-digit basin level, which were compiled by aggregating county-level survey data collected by the Conservation Technology Information Center (CTIC)[33]. These data were disaggregated to the 12-digit subbasin level, within a given 8-digit basin, in a manner that maintained the same distribution of tillage types as reported at the 8-digit basin level, to the extent possible. Each tillage type was represented by an appropriate number of tillage passes (and corresponding levels of crop residue incorporation), as well as appropriate values of Manning's roughness coefficient for overland flow (OV_N) and crop cover factor (USLE_C), which are used in the MUSLE within SWAT to estimate water-induced soil erosion[25].

Regional estimates of the distribution of other conservation practices were not publicly available at the time of this study. To address this deficiency we used a proxy approach that was based on information provided in the Conservation Effects Assessment Project (CEAP)[11,34] OTRB study (USDA-NRCS, 2011). They reported that a significant part of the cropland in the OTRB had at least one in-field conservation practice (terrace, strip-cropping, contouring), while highly erodible land was managed to a much greater extent compared to less erodible areas. In our model the conservation practices were likely to be present in all the HRUs due to their relatively large areas (12-digit subbasins). Therefore, we simulated the effect of in-field conservation practices on erosion control in all HRUs by reducing the management (P) factor of the MUSLE[22,25], which was the major parameter that governed the representation of all such practices in the model[24]. Similarly, we reduced the slope length to represent the effects of terraces. However, slope lengths were not adjusted for HRUs with slopes less than 2.3% because estimated erosion has been found to be inversely correlated with slope length for such lower slopes[24]. We specified higher reductions of the management P factor in high-sloping agricultural HRUs and slight reductions in low sloping ones. These adjustments of the P factor had also the purpose of forcing the model to predict reasonable sediment yields. Adjustment of curve numbers (CNs), which are additionally used to represent such practices[24], was not implemented because the CNs served as one of the key parameters for calibrating the hydrological OTRB model (see next subsection). The reduced CN values that resulted from the flow calibration during the final 15-year period coincided with the historical period of expanded adoption of conservation tillage and other conservation practices in the OTRB region, which likely resulted in increased infiltration of precipitation and reduced surface runoff per findings in

previous studies[35,36].

Fertilizer (including manure) application rates were calculated based on recent nutrient balance estimates at the 8-digit level obtained from the Nutrient Use Geographic Information System (NuGIS) for the U.S.[37]. However, problems were encountered in applying these data in the current modeling system due to uncertainty in the fertilizer sales data used in NuGIS and other factors. Thus, statewide averages computed from the NuGIS data were used in the present study, resulting in annual average N and P rates applied to cropland that ranged between 117-156 kg/hm$^2$·a and 25-34 kg/hm$^2$·a, respectively, with N applied only to corn. For hay and pastureland we used the auto-fertilization routine of SWAT by setting 70 kg/hm$^2$·a (N) as the maximum limit.

Monthly streamflow data obtained from 5 OTRB USGS stations (Figure 3) were used for calibrating the model[20], with the most downstream station located at Metropolis, Illinois. These data were obtained for 1975 to 2010, with the most recent 14-year period used for calibration and the rest for validation. In-stream sediment, nitrate-N ($NO_3$-N), organic N, and organic and mineral P data were available for most of these stations on a monthly basis for similar or shorter time-periods. Calibration of river sediment and nutrient yields was also conducted for all the locations with available data after incorporating N and P loads from thousands of point sources across the region[38,39].

### 2.4 Model performance and evaluation

The hydrologic calibration of the OTRB was conducted with the use of the SWAT-CUP software package[40]. SWAT-CUP offers a semi-automatic or combined manual/automatic calibration of SWAT projects, allowing the user to control the range of parameter perturbations in seeking to identify their optimum values. Parameters can range either by a percentage from their initial values or within predefined lower and upper bounds. The Sequential Uncertainty Fitting (SUFI-2) algorithm[41] was used in this study, which is the most efficient option for large regional applications[42,43] and is highly recommended for the calibration of SWAT simulations[44].

The calibration of the OTRB model with SUFI-2 was conducted on a monthly basis using the most recent 14-year period of observed flows (1997 to 2010). To make the process feasible with respect to total time needed for thousands of iterations (SWAT runs), we first created SWAT projects for each of the subbasins upstream of the monitoring points (Figure 3) excluding Cannelton and Metropolis, which were downstream of upstream areas with monitoring sites (Figure 3). Each of the three 'hydrologically independent' subregions corresponded to either the most upstream part of the main stem (Ohio River) or a major tributary flowing into it (i.e., the Wabash and Tennessee Rivers). Each parameterized sub-project was manipulated by the SWAT-CUP interface for auto-calibration and uncertainty analysis with SUFI-2. This study used eight parameters (Neitsch et al. 2009): five related to groundwater (ALPHA_BF, GW_DELAY, GWQMN, RCHRG_DP and GW_REVAP), the curve number (CN2), the soil evaporation compensation coefficient (ESCO) and the available soil water capacity of the first soil layer (SOL_AWC(1)), in order to calibrate 3 individual SWAT projects within 500 iterations (runs). The SOL_AWC(1) and CN were the only parameters allowed to vary by a percentage from the default value (±20%), while all others were modified with absolute values within realistic ranges. All projects were executed simultaneously in a personal computer (PC) with 32 thread processors and 128 GB RAM. The next step was to keep the calibrated values within all the upstream subbasins and calibrate the same eight parameters of the intermediate, still uncalibrated areas above Cannelton and Metropolis consecutively.

The nutrient calibration was executed by using a manual approach in which important water quality parameters were adjusted in SWAT[12]. As previously mentioned, the management factor (USLE_P) of the MUSLE equation was the primary driving factor of controlling erosion simulation and sediment delivery to streams. River nutrient yields were calibrated based on several other parameters that govern nutrient soil availability and cycling. Some of them were the N and P percolation coefficients (NPERCO, PPERCO), the concentrations of organic forms of N and P in soil at the

beginning of the simulation (SOL_ORGN and SOL_ORGP) as well as the coefficients governing denitrification[25].

It should be noted that upland erosion and nutrient outputs from agricultural fields were not directly measurable variables. Pollutant yields were measured and reported along streams and rivers, while the official USGS data corresponded to a lower total N and P load on a 'per ha of the upstream area' basis at Metropolis, Illinois compared to the upland pollution from agricultural fields analyzed by our results. This was mainly attributed to the unit area contribution of non-agricultural areas to water pollution, which was much lower than that of the agricultural land. The reliability of predictions from the agricultural land was based on the ability of SWAT to capture spatial heterogeneity given the accuracy of our model parameterization and the success of the calibration process. However, even though there is some uncertainty regarding the predicted absolute values, the purpose of the study at this point is to analyze relative comparisons of the productivity and the susceptibility of the agricultural land in pollutant loss under various management and climatic conditions.

The results of the hydrologic and pollutant calibration/validation simulations were evaluated according to the percent bias (PBIAS), the coefficient of determination ($R^2$) and the Nash-Sutcliffe (NS) modeling efficiency[45,46] and other indices not reported here. Statistical results for the streamflow and two pollutant indicators ($NO_3$-N and Total P (TP)) are listed for the five monitoring sites (Figure 3) in Tables 1 and 2, respectively, for both the calibration (1997-2010) and validation (1975-1996) periods. The majority of the statistics were satisfactory or better per suggested criteria[45] for judging hydrologic and water quality model results although the TP results were distinctly weaker, reflecting greater uncertainty in those estimates. Comparisons of simulated versus measured monthly streamflow, $NO_3$-N and TP are plotted in Figures 4 to 6. These results indicate that SWAT accurately replicated these indicators although there is a trend towards overprediction of the nutrient load peaks, especially for TP. A complete description of the OTRB calibration/validation methods and results of the OTRB model are reported in a previous study[12].

**Table 1 Monthly calibration (1997-2010) and validation (1975-1996) OTRB streamflow statistical results (monitoring locations are shown in Figure 3)**

| Monitoring location | Subbasin | USGS station | Calibration | | | Validation | | |
|---|---|---|---|---|---|---|---|---|
| | | | $R^2$ | NS | PBIAS | $R^2$ | NS | PBIAS |
| Paducah | Ohio | 03216600 | 0.82 | 0.77 | 12.74 | 0.86 | 0.71 | 27.17 |
| Greenup | Tennessee | 03609500 | 0.90 | 0.89 | -5.25 | 0.87 | 0.87 | 3.40 |
| Mt.Carmel | Wabash | 03377500 | 0.83 | 0.82 | -3.47 | 0.74 | 0.68 | -1.48 |
| Cannelton Dam | Ohio | 03303280 | 0.92 | 0.92 | -1.38 | 0.89 | 0.89 | 2.14 |
| Metropolis | Ohio | 03611500 | 0.90 | 0.89 | 6.87 | 0.88 | 0.83 | 14.42 |

**Table 2 Monthly calibration (1997-2010) and validation (1975-1996) OTRB water quality statistical results (monitoring locations are shown in Figure 3)**

| Monitoring location | $NO_3$-N statistical results | | | | | | TP statistical results | | | | | |
|---|---|---|---|---|---|---|---|---|---|---|---|---|
| | Cal | Val | Cal | Val | Cal | Val | Cal | Val | Cal | Val | Cal | Val |
| | PBIAS | PBIAS | NS | NS | $R^2$ | $R^2$ | PBIAS | PBIAS | NS | NS | $R^2$ | $R^2$ |
| Paducah | -8.32 | 22.76 | 0.56 | 0.68 | 0.57 | 0.73 | -12.14 | 4.71 | -0.17 | -0.07 | 0.24 | 0.61 |
| Greenup | 12.28 | 24.07 | 0.61 | 0.46 | 0.73 | 0.74 | 9.70 | 35.38 | 0.54 | 0.29 | 0.53 | 0.45 |
| Mt.Carmel | 0.47 | -28.73 | 0.60 | -0.55 | 0.66 | 0.62 | -5.56 | 15.52 | 0.06 | 0.31 | 0.53 | 0.55 |
| Cannelton Dam | 1.99 | 17.77 | 0.76 | 0.70 | 0.77 | 0.77 | 20.77 | 25.30 | 0.51 | 0.42 | 0.58 | 0.46 |
| Metropolis | -4.90 | 12.49 | 0.72 | 0.61 | 0.75 | 0.63 | -7.64 | -0.51 | 0.37 | 0.36 | 0.49 | 0.44 |

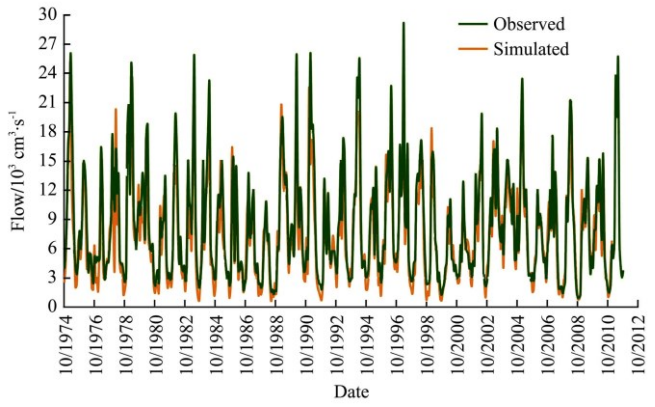


Figure 4 Simulated versus observed streamflows at the Ohio River outlet (Metropolis IL; Figure 3) for both calibration (1997-2010) and validation (1975-1996) periods

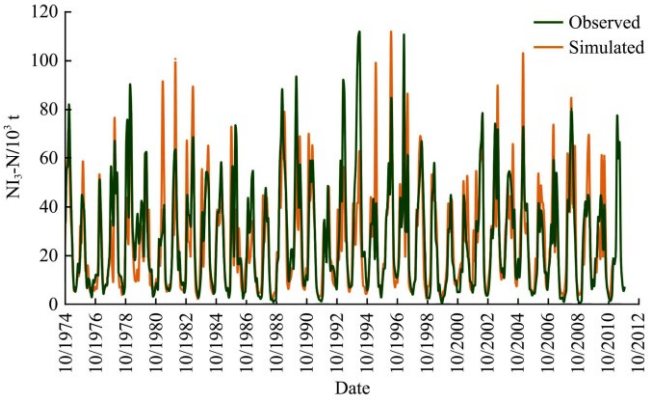


Figure 5 Simulated versus observed nitrate-N loads at the Ohio River outlet (Metropolis, IL; Figure 3) for both calibration (1997-2010) and validation (1975-1996) periods

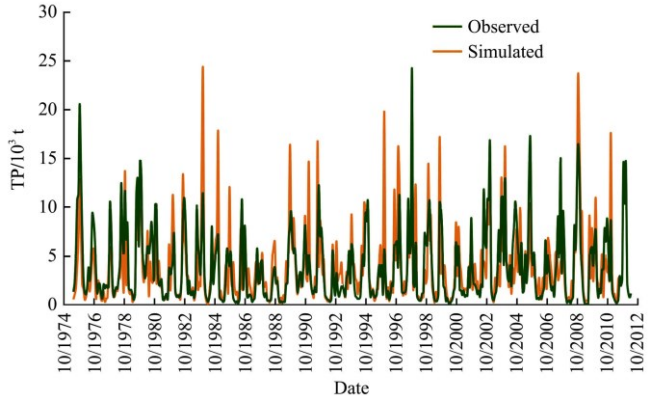


Figure 6 Simulated versus observed TP loads at the Ohio River outlet (Metropolis, IL; Figure 3) for both calibration (1997-2010) and validation (1975-1996) periods

### 2.5 General circulation model (GCM) and predicted mid-century climate

Climate projections were taken from results of coupled atmosphere-ocean general circulation models (GCMs) that participated in the World Climate Research Programme Coupled Model Intercomparison Project phase 3 (CMIP3)[47]. Although newer results are now available from models participating in phase 5 of that project (i.e., CMIP5)[48] we restrict our analysis to CMIP3 models for consistency with our prior related research for the Upper Mississippi River Basin (UMRB)[49]. In addition, it has been found in previous research that the patterns of temperature and precipitation change are quite similar between the CMIP3 and CMIP5 models[50].

We used all CMIP3 GCMs for which the necessary output fields were available in the standard data archive. The most common reason for excluding a model was that it did not archive a near-surface humidity variable. Even though the available models were less than half of those participating in CMIP3, they have equilibrium climate sensitivity (ECS) ranging from the lowest value in the CMIP3 ensemble (for INM-CM3.0) to tied for highest (IPSL-CM4). Therefore, at least in this respect the models we have used span the range of projections in CMIP3. The models used, their horizontal grid spacings and ECS (where known) are summarized in Table 3. Table 3 also lists the transient climate response (TCR), which is the warming around the time that carbon dioxide has doubled from its pre-industrial value but before the system has adjusted to slow feedbacks. Although ECS is probably a more widely-known model characteristic, TCR may be a more appropriate measure given that our period of interest (2046-2065) is around the time of $CO_2$ doubling before the system has equilibrated to all feedbacks[51,52].

Current climate is taken as the years 1981-1999 from each model's results for CMIP3 "Climate of the 20th Century" simulations (for models that performed more than one run the first ensemble member was used). These simulations included observed forcings from greenhouse gases, natural and anthropogenic aerosols, solar variability, ozone and land use changes for the period 1900-2000. For future climate we use each model's results for the years 2046-2065 from A1B climate scenario. This scenario specifies that emissions of the major greenhouse gases (carbon dioxide, methane and nitrous oxide) increase through the middle of the 21st century and stabilize or decline thereafter, with carbon dioxide concentrations stabilizing at $720\times10^{-6}$ *V*. Solar radiation and volcanic aerosols are held at their 2000

values throughout the 21st century. An overview of the CMIP3 experiment design is given elsewhere[54].

For temperature and precipitation we used monthly downscaled results[47] that were created for each of the GCMs in Table 3. The downscaling method used was bias correction with spatial disaggregation (BCSD). This method removes precipitation and temperature biases for each of the model projections in the present climate through quantile matching, then interpolates forecast anomalies for a given monthly time step to a 1/8 degree latitude-longitude grid and superimposed on the observed baseline climate. Future values of other variables required by SWAT (monthly solar radiation, dew point and wind speed) were generated by superimposing the difference between each GCM's future (2046-2065) and current (1981-2000) climate onto observed historical records; this is the widely used "delta" (also called "change factor") method. Further details regarding the BCSD approach and other aspects of inputting the climate projections in SWAT are described in previous research[49].

**Table 3 Name, institutional information, country of origin, grid spacing, and ECS and TCR data for the seven global circulation models (GCMs) used for the OTRB climate change analyses**

| Model | Institution | Country | Grid spacing[a] | ECS (TCR)[b] |
|---|---|---|---|---|
| BCCR-BCM2.0 | Bjerknes Centre for Climate Research | Norway | T63 (1.9°×1.9°) | na |
| CGCM3.1 | Canadian Centre for Climate Modelling and Analysis | Canada | T47 (2.5°×2.5°) | 3.4 (1.9) |
| CNRM-CM3 | Météo-France/Centre National de Recherches Météorologiques | France | T63 (1.9°×1.9°) | na (1.6) |
| INM-CM3.0 | Institute for Numerical Mathematics | Russia | 4°×5° | 2.1 (1.6) |
| IPSL-CM4 | Institut Pierre Simon Laplace | France | 2.5°×3.75° | 4.4 (2.1) |
| MIROC3.2 (medres) | University of Tokyo, National Institute for Environmental Studies, and Frontier Research Center for Global Change | Japan | T42 (2.8°×2.8°) | 4.0 (2.1) |
| MRI-CGCM2.3.2 | Meteorological Research Institute | Japan | T42 (2.8°×2.8°) | 3.2 (2.2) |

Note: [a] Grid spacing is the latitude-by-longitude spacing of the computational grid, or the spectral truncation and near-equatorial latitude-by-longitude spacing of the corresponding Gaussian grid for spectral models.

[b] ECS and TCR are equilibrium climate sensitivity and transient climate response in units of K[53], with "na" indicating values are not available.

## 2.6 Agricultural management scenarios

Three agricultural management scenarios were selected, formulated and tested with SWAT under the existing and future climate conditions in OTRB in order to compare their effects on pollutant losses from land to surface waters as well as their ability to sustain crop production. The implementation of these scenarios is of high interest within the CSCAP Corn Belt Region initiative and are similar to the management scenarios that were simulated for the UMRB[49]. The land use and cropping management scenarios included expansion across all OTRB cropland of: (1) continuous corn rotation (C-C), (2) no-tillage (NT) and (3) planting of rye as a winter cover crop in alternating years between row crop growing seasons in the C-S and C-C rotations. The C-C scenario represents a bioenergy scenario in which demand for corn grain-based ethanol increases greatly in the future. The other two scenarios depict expansions of cover crops and no-tillage which are both viable conservation practices; cover crops are effective in controlling sediment and nutrient losses[55,56] while no-tillage is effective at controlling sediment losses and some forms of nutrient losses[57-59]. Table 4 summarizes the specific implementation of each of these scenarios in SWAT.

**Table 4 Management scenarios implemented in the agricultural land of the OTRB**

| Scenario | Implementation in rotations | Implementation in SWAT | Main Purpose |
|---|---|---|---|
| Continuous corn (C-C) | To all C-S rotations of the baseline in OTRB | Changing soybean with corn and increasing N fertilization by 50 $kg \cdot hm^{-2} \cdot a^{-1}$ [a] | Increase corn production in the long-term |
| No-tillage (NT) | To all C-S and C-C rotations with conventional, reduced or mulch tillage | Apply tillage passes with lower depth (25 mm) and low mixing efficiency (0.05) and reduce the crop cover factor (USLE_C)[b] in the crop database. Reduce CN values and increase OV_N[b] | Reducing erosion, N and P losses from fields to waters |
| Cover crop (Rye) | To all C-S and C-C rotations in the OTRB | Plant rye as a winter cover crop (Oct-April) between row crops in both the C-S and C-C rotations | Reducing erosion, N and P losses from fields to waters |

Note: [a] The unit "a" denotes annual or year.

[b] The USLE_C and OV_N parameters refer to the Universal Soil Loss Equation crop cover and Manning's roughness coefficient for overland flow, respectively, as described in more detail in the SWAT model documentation[25].

## 3 Results and discussion

### 3.1 Water balance under the historical and future climate

The calibrated SWAT-OTRB model was executed with the current (1981-2000) and future (2046-2065) climate data. Table 5 summarizes the mean annual water balance in the basin. On average, annual precipitation in the future climate ranged from a maximum of 1 296 mm in the CNRM-CM3 projection to a minimum of 1 046 mm in the MIROC3.2 (medres) projection. This corresponds to precipitation changes from +10% to -11% relative to current climate. An important finding, however, is that even the projections which predict precipitation decrease on an annual basis result in precipitation increase during the colder period of the year (Nov-March). This can be clearly observed in Table 6, where average monthly precipitation changes from the historic climate are summarized for all projections. On the other hand, the majority of projections predict a reduction in precipitation within the warmer period between April and October as shown in Table 6 with possible implications to crop production. Moreover, there is a consistent snowfall decrease predicted for all of the future scenarios (Table 5) and months of the year (Table 7). This was clearly caused by a consistent increase in temperature across all of the GCMs given the fact that precipitation was increased in all the cold months when snowfall can occur. The latter implies that increases in PET and actual ET are also expected; however, all models except the one with lowest precipitation show virtually no change or very slight increases (up to 2.9%) in annual ET. This result occurs because most of the GCMs predicted higher temperature increases within the cooler part of the year with direct impact on snowfall but lower increases (or even decreases)

**Table 5 Mean annual simulated water balance components in the OTRB for the period 1981-2000 or 2046-2065 under the historic and seven GCMs and the baseline agricultural management with the common C-S and S-C rotations under several tillage systems and no cover crops growing**

| Climate Scenario | Water Balance Indicators/mm | | | | | |
|---|---|---|---|---|---|---|
| | Precipitation | Snowfall | Surface runoff | Total runoff | ET | PET |
| Baseline climate | 1175 | 78 | 151 | 448 | 649 | 1032 |
| BCCR_BCM2.0 | 1189 | 45 | 141 | 448 | 663 | 1089 |
| CGCM3.1 | 1228 | 50 | 157 | 491 | 656 | 1053 |
| CNRM-CM3 | 1296 | 62 | 185 | 549 | 663 | 1074 |
| INM-CM3.0 | 1136 | 60 | 132 | 396 | 663 | 1142 |
| IPSL-CM4 | 1195 | 29 | 137 | 448 | 668 | 1115 |
| MIROC3.2 (medres) | 1046 | 38 | 106 | 359 | 617 | 1075 |
| MRI-CGCM2.3.2 | 1248 | 49 | 163 | 524 | 642 | 997 |

**Table 6 Average monthly precipitation change from the historic climate predicted within each GCM projection for the 20-year future period of 2046-2065** mm

| Month | Historic Climate Precipitation | BCCR_BCM2.0 | CCG CM3.1 | CNRM-CM3 | INM-CM3.0 | IPSL-CM4 | MIROC3.2 (medres) | MRI-CGCM2.3.2 |
|---|---|---|---|---|---|---|---|---|
| November | 102.14 | -0.47 | 26.76 | 7.66 | -3.63 | 27.80 | -2.52 | 4.56 |
| December | 99.48 | 2.25 | 24.84 | 5.58 | -4.32 | 13.30 | 7.93 | -4.17 |
| January | 85.66 | 6.87 | 3.49 | -0.48 | 29.14 | -2.19 | -14.10 | 17.40 |
| February | 91.05 | 0.80 | -4.96 | 29.42 | 0.66 | 8.98 | 11.49 | 6.07 |
| March | 102.86 | 22.41 | 6.03 | 28.91 | 1.61 | 10.78 | 8.97 | 22.88 |
| April | 102.20 | 1.04 | 8.23 | 3.20 | -7.09 | -10.69 | 6.50 | 5.12 |
| May | 123.19 | 12.26 | -2.59 | 22.71 | -16.20 | -12.62 | -30.47 | -3.11 |
| June | 109.37 | -10.36 | 4.24 | 20.26 | -28.53 | -6.91 | -28.71 | -12.72 |
| July | 110.84 | -1.35 | -9.71 | -10.19 | -10.25 | 9.36 | -35.30 | 7.00 |
| August | 90.63 | -6.68 | 8.48 | 7.20 | 5.91 | -1.01 | -19.77 | 6.09 |
| September | 83.28 | -15.63 | -2.75 | -1.13 | 10.29 | -19.67 | -23.37 | 16.39 |
| October | 76.29 | 3.39 | -9.05 | 8.88 | -16.50 | 3.05 | -9.42 | 7.85 |
| Year | 1177.00 | 14.50 | 53.00 | 122.00 | -38.90 | 20.20 | -128.80 | 73.40 |

**Table 7 Average monthly precipitation change from the historic climate predicted within each GCM projection for the 20-year future period of 2046-2065** mm

| Month | Historic climate snowfall | BCCR_BCM2.0 | CCG CM3.1 | CNRM-CM3 | INM-CM3.0 | IPSL-CM4 | MIROC3.2 (medres) | MRI-CGCM2.3.2 |
|---|---|---|---|---|---|---|---|---|
| November | 3.76 | -2.3 | -2.0 | -2.5 | -2.3 | -2.8 | -3.1 | -2.0 |
| December | 17.62 | -8.0 | -4.2 | -2.6 | -7.8 | -10.9 | -8.0 | -7.7 |
| January | 25.35 | -11.1 | -5.3 | -8.0 | 2.6 | -13.3 | -11.4 | -7.8 |
| February | 19.43 | -6.1 | -8.8 | 1.1 | -3.2 | -13.4 | -9.6 | -6.9 |
| March | 10.25 | -4.2 | -6.6 | -2.8 | -6.0 | -7.2 | -6.2 | -3.6 |
| April | 1.67 | -1.2 | -1.2 | -0.8 | -1.4 | -1.4 | -1.3 | -1.0 |
| May | 0.01 | 0.0 | 0.0 | 0.0 | 0.0 | 0.0 | 0.0 | 0.0 |
| June | 0.00 | 0.0 | 0.0 | 0.0 | 0.0 | 0.0 | 0.0 | 0.0 |
| July | 0.00 | 0.0 | 0.0 | 0.0 | 0.0 | 0.0 | 0.0 | 0.0 |
| August | 0.00 | 0.0 | 0.0 | 0.0 | 0.0 | 0.0 | 0.0 | 0.0 |
| September | 0.00 | 0.0 | 0.0 | 0.0 | 0.0 | 0.0 | 0.0 | 0.0 |
| October | 0.16 | -0.1 | -0.2 | -0.2 | -0.2 | -0.2 | -0.2 | -0.2 |
| Year | 78.30 | -33.2 | -28.2 | -15.7 | -18.1 | -49.2 | -39.7 | -29.1 |

of temperature in the warmer part (including the crop-growth periods), which in combination do not result in considerably altered annual PET and ET values. On the other hand, mean annual runoff predicted by the GCMs manifested greater deviation as compared to the baseline climate, ranging from a 27.5% increase for the model with highest annual precipitation to a 19.9% decrease for the model with lowest annual precipitation. This shows that runoff production is generally driven by water inputs into the basin following the precipitation differences between the GCMs.

Figures 7 and 8 summarize the monthly variations of simulated surface runoff and ET simulated for the baseline and predicted climate with SWAT. The baseline runoff is highest in February and March, and lowest in early autumn. It is interesting to note that monthly surface runoff values followed a similar pattern for all seven GCM projections. The CRNM_CM3 GCM resulted in the highest monthly values for most months except in late summer and autumn, leading to the highest annual surface runoff as shown in Table 5. In contrast, the MRI-CGCM2.3.2 GCM resulted in the highest increase in runoff compared to the baseline during summer and autumn, which coincided with the crop-growing cycle. Most GCM projections generated reduced runoff during this period (June-September), which was driven by reduced precipitation. This finding indicates that the future climate scenarios tested in this study could cause increased water stress to crops grown in the eastern Corn Belt. Another key finding is that most GCM scenarios resulted in large surface runoff increases during winter which could exacerbate the risk of flooding in susceptible areas.

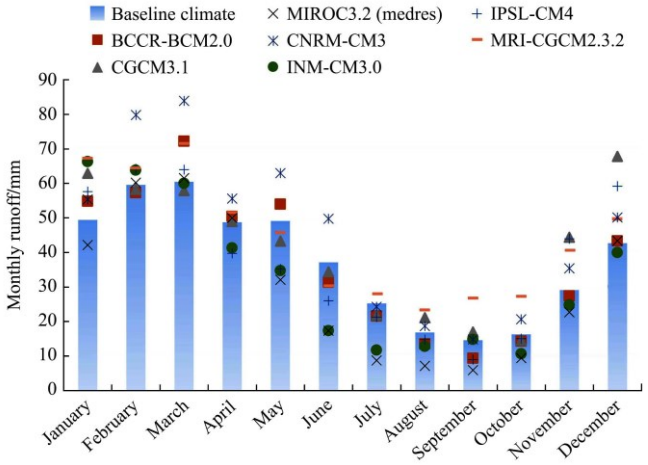


Figure 7 Mean monthly runoff (mm) simulated for the entire OTRB in response to the baseline climate (1981-2000) and future (2046-2065) GCM climate projections (baseline values are represented by columns)

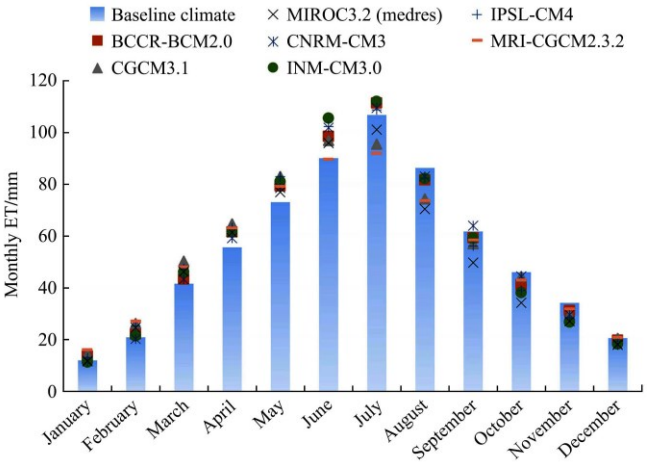


Figure 8 Mean monthly actual Evapotransporation (ET; mm) simulated for the entire OTRB in response to the baseline climate (1981-2000) and seven future (2046-2065) GCM climate projections (baseline values are represented by columns)

Maximum baseline ET was predicted to occur within the growing period, especially during summer, by all seven GCM projections (Figure 8). It is also of interest to note the small ET differences amongst the GCMs for most months. Almost all of the predicted GCM ET values were higher than the baseline ET in spring and summer and lower from midsummer until the end of autumn, yielding the small changes in annual ET discussed previously. Increased ET during winter was driven by increased temperatures, which reduced snowfall (and thus snow cover) in the basin (Tables 5 and 7). Decreased ET within the second phase of crop growth (July-October) is attributed primarily to reduced precipitation within this period rather than to reduced temperatures. In general, the consistent trend of reduced ET within this period predicted by the GCMs implies reduced net water consumption by plants and thus a potential loss of production to predicted future mid-century climate change in OTRB.

### 3.2 Pollutant losses from scenarios implementation

In our calibrated SWAT-OTRB model, sediment losses were predicted to average 1.6 t/hm$^2$·a from agricultural lands during the 20-year baseline period (1981-2000). Baseline TN and TP losses were predicted to be 22.7 and 1.95 kg/hm$^2$·a, respectively, from agricultural lands.

Figure 9 shows the mean annual sediment yields generated from the OTRB agricultural land for both the current and predicted climates, as well as for the implementation of both the baseline management scenario and the three scenarios listed in Table 4. The C-C scenario resulted in slightly reduced sediment from HRUs compared with the baseline (Figure 9). Although corn was erodible to the same extent as soybean according to the attributes of both crops in SWAT (USLE_C factor, CN values), the replacement of soybean with corn produces higher residue amounts, resulting in reduced soil erosion. The expansion of NT was the most promising scenario, which resulted in drastic sediment and P load reduction from the agricultural land. Sediment reduction approached 70% under the historic climate compared to the baseline agricultural management. The establishment of rye as a winter cover crop within the traditional OTRB rotations (C-S or C-C) resulted in reduced sediment of 35% to 40%, because of increased soil protection. Under the future climates all agricultural management scenarios behaved similarly, following a consistent trend with reference to the baseline agricultural management.

In general, the predicted sediment losses were relatively split in response to the future climate projections with four GCMs resulting in greater sediment losses as compared to the baseline versus the other three GCMs that generated lower sediment losses relative to the baseline. Due to these variations the average GCM sediment predictions (average value of the seven GCMs) are very close to the sediment yields predicted under the historic climate for all of the management scenarios (Figure 9). This highlights the variability between climate projections, which may result in different trends in climate and water pollution levels, adding complexity to evaluating future impacts on water resources under climate change and emphasizing the need to consider a range of climate projections in order to avoid misleading results.

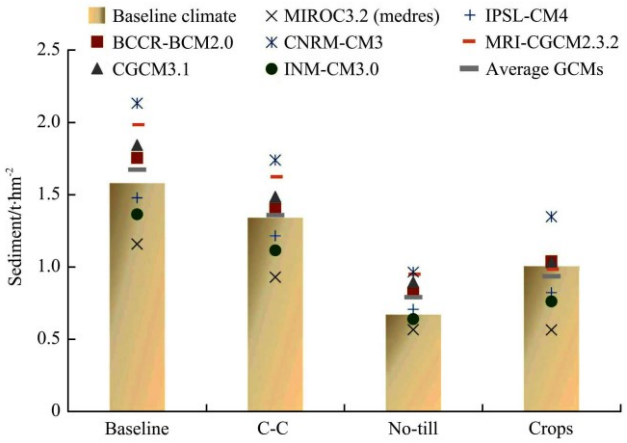


Figure 9 Average annual sediment losses from the cropland of the OTRB for the baseline management and three agricultural management scenarios, in response to the baseline climate (1981-2000), seven individual future (2046-2065) GCM climate projections and the average of the GCM projections (the sediment losses generated by the baseline climate are represented by the columns)

Figure 10 and Figure 11 present the mean annual TP and TN losses to waters from the agricultural land of OTRB for the four agricultural management scenarios and nine climate scenarios: baseline climate, the seven future GCM projections and the average of the seven projections. The conclusions drawn for the TP and TN

losses for all of the combined climate/agricultural scenarios are similar to the previously described sediment results (Figure 9). However, the results indicated that by substituting soybean with corn in the C-C scenario, the application of additional P on the corn caused an increase in P losses which are greater than the reduction in P losses from the reduced erosion. A similar response also occurred for the TN losses, due to the increased application of N in the C-C scenario, resulting in the increased N applications muting some of benefit of the reduced sediment losses. However, the overall predicted impact still resulted in a slight reduction of TN in the C-C scenario as compared to the baseline.

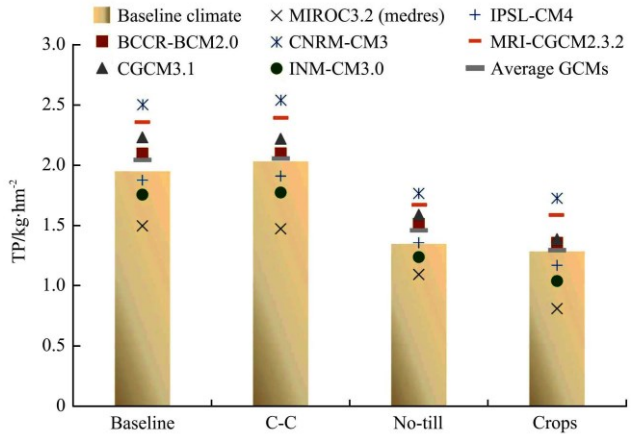


Figure 10 Average annual total phosphorus (TP) losses from the cropland of OTRB for the baseline management and three agricultural management scenarios, in response to the baseline climate (1981-2000), seven individual future (2046-2065) GCM climate projections and average of GCM projections (TP losses generated by the baseline climate are represented by columns)

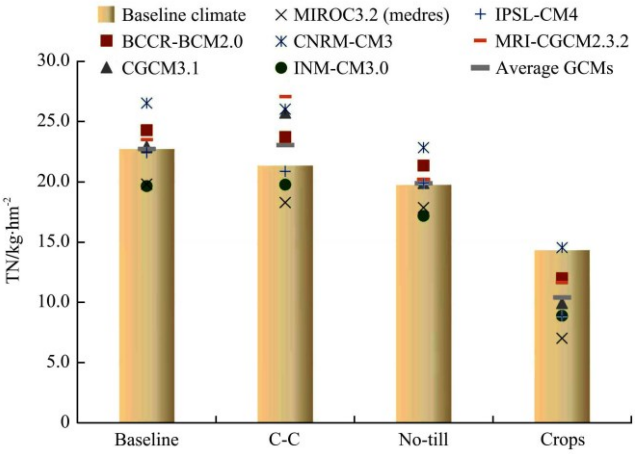


Figure 11 Average annual total nitrogen (TN) losses from the cropland of the OTRB for the baseline management and three agricultural management scenarios, in response to the baseline climate (1981-2000), seven individual future (2046-2065) GCM climate projections and the average of GCM projections (TN losses generated by the baseline climate are represented by columns)

All seven GCMs produced qualitatively similar results under the four management practices, with no-till and cover crops resulting in the lowest losses. The TN losses, mainly comprised by $NO_3$-N, were highly governed by subsurface flow pathways (tile and baseflow) and thus manifested greater declines in response to the climate projections of reduced precipitation and runoff. However, increased nitrogen fertilization of 50 kg/hm$^2$·a N during each year of C-C corn cultivation counteracted the reductions of sediment-related N forms, leading to virtually identical TN losses as compared to the baseline management. Cover crops were predicted to be the most effective practice in reducing N losses, with almost all of the GCM scenarios resulting in TN loads that were lower than those of the historic baseline climate.

### 3.3 Predicted yields from scenarios implementation

Table 8 summarizes the SWAT crop yield results for corn and soybean under all combinations of scenarios. Mean annual simulated corn and soybean yields in the baseline scenario were 7.8 and 2.8 t /hm$^2$·a, respectively, across the agricultural land of the OTRB. An increased average annual corn yield occurred for the continuous corn (C-C) scenario, due to the increased nitrogen fertilization. However, the average corn yield was calculated over 20 years for the C-C scenario, which may have had some statistical impact, because the corn production years were double those simulated in the baseline (10 years of corn). On the other hand, NT applied in all C-S and C-C HRUs of OTRB did not have any impacts on yield. The results can however be considered promising as the practice was able to sustain yields under the new residue management conditions. Finally, increased corn yields were predicted for the cover crop scenario, which was not the case for soybean where a very slight decrease was produced. The increased corn productivity here is attributed to the reduced nutrient losses to waters due to the coverage of the ground with the cover crop. However, it has been documented that the use of rye cover crops can have allelopathic effects on corn, resulting in reduced corn yields in some circumstances[60,61]. SWAT is not able to capture these allelopathic effects.

**Table 8 Mean annual OTRB simulated crop yields for the baseline climate (1981-2000) or future (2046-2065) GCM climate projections, and the four agricultural management scenarios**

| Climate Scenarios | Corn yields ($t \cdot hm^{-2}$) | | | | Soybean yields ($t \cdot hm^{-2}$) | | | |
|---|---|---|---|---|---|---|---|---|
| | Baseline | C-C | No-till | Cover crops | Baseline | C-C | No-till | Cover crops |
| Baseline climate | 7.79 | 8.33 | 7.79 | 8.44 | 2.82 | 0.00 | 2.82 | 2.76 |
| BCCR_BCM2.0 | 7.21 | 7.95 | 7.21 | 7.98 | 2.52 | 0.00 | 2.52 | 2.48 |
| CGCM3.1 | 6.67 | 7.42 | 6.67 | 7.22 | 2.09 | 0.00 | 2.09 | 2.06 |
| CNRM-CM3 | 7.25 | 7.96 | 7.25 | 8.06 | 2.57 | 0.00 | 2.57 | 2.53 |
| INM-CM3.0 | 7.36 | 8.10 | 7.36 | 7.92 | 2.38 | 0.00 | 2.38 | 2.35 |
| IPSL-CM4 | 7.38 | 8.21 | 7.38 | 8.13 | 2.51 | 0.00 | 2.51 | 2.47 |
| MIROC3.2 (medres) | 7.45 | 8.25 | 7.45 | 8.20 | 2.51 | 0.00 | 2.51 | 2.47 |
| MRI-CGCM2.3.2 | 6.62 | 7.32 | 6.63 | 7.21 | 2.09 | 0.00 | 2.09 | 2.07 |

The predicted corn and soybean yields under all future climates and the four agricultural management scenarios consistently declined with reference to the baseline climate conditions, consistent with the analysis of the mean annual water balance components showing reduced ET in the second half of the crop growth period. Decreased yields are thus attributed to the decreased precipitation during the crucial phase of the crop growth cycles, which resulted in water stress in the cropland areas. Note that the lowest simulated yields are obtained with two GCMs having significant predicted increase in annual precipitation (MRI-CGCM2.3.2 and CGCM3.1). This illustrates that changes in crop yields depend critically on timing of precipitation, not necessarily on changes to annual values or on the timing of temperature (and thus ET) changes, which coincides with the very critical crop-growth stage of July-August in the case of these two projections (Figure 8).

## 4 Conclusions

This study examined the impact of three agricultural management scenarios in the agricultural land of the OTRB region for both current climate conditions and various climate change projections generated with seven GCMs for a future mid-century time period (2046 to 2065). All management scenarios behaved similarly under the historical and future climates, generally resulting in reduced erosion and nutrient loadings to surface water bodies compared to the baseline agricultural management, with cover crops causing the highest water pollution reduction. The trend of the simulated effects of the scenarios tested was in general agreement with findings from several recently reported experiments[62]. The predicted corn and soybean yields in the region were not influenced negatively by the agricultural management scenarios that were simulated using the baseline climate.

Both water quality and crop yield numbers under the seven GCMs deviated considerably from those of the baseline climate. The analysis of the results revealed that corn and soybean yields decreased by up to 20% on a mean annual basis in response to the GCM scenarios, while water quality alterations were either positive or negative depending on the GCM. By examining SWAT results under various climate projections, consistent findings on productivity under various future climate conditions increase the certainty of these predictions. On the other hand, high fluctuations in predicted sediment and nutrient exports in response to the different GCM projections reveal considerable uncertainty in the future predictions. These results demonstrate that results from a single GCM are not robust, and that a range of GCMs should be used when projecting impacts of climate change.

This study highlights the capabilities of SWAT in connecting agricultural management strategies with hydrologic-process simulations at the river basin scale. It also supports its use as a component of an integrated decision support system for the complex Corn Belt agricultural systems. Such tools can provide scientifically based estimates of the effect of a wide array of alternative cropping and management strategies under different climatic conditions, enabling informed choices affecting environmental and economic sustainability of

the region in the coming decades. Overall, the study highlights the loss of productivity in the eastern Corn Belt under climate change and the value of SWAT as a tool to analyze the effects of climate change on several parameters of interest at the basin scale.

The conclusions drawn here were based on an analysis of water quantity and quality variables at the large basin scale. It would be useful to analyze the results by mapping the effectiveness of each scenario in reducing pollution and in sustaining crop yields at the 12-digit subbasin level. However, improved representation of existing conservation practices, nutrient application rates, and other management practice aspects are needed in order to simulate accurate combinations of practices across specific landscapes. A practice allocation across the landscape of OTRB would also require a clear cost estimation of the practices in different locations. In addition, incorporation of HRUs within the 12-digit subbasins is needed to better represent the impacts of different combinations of cropland landscapes and management practices.

## Acknowledgements

This research was partially funded by the National Science Foundation, Award No. DEB1010259, Understanding Land Use Decisions & Watershed Scale Interactions: Water Quality in the Mississippi River Basin & Hypoxic Conditions in the Gulf of Mexico, and by the U.S. Department of Agriculture, National Institute of Food and Agriculture, Award No. 20116800230190, Climate Change, Mitigation, and Adaptation In Corn-Based Cropping Systems.

## [References]

[1] USEPA SAB. Hypoxia in the northern Gulf of Mexico: an update by the EPA Science Advisory Board. EPA-SAB-08-004. Washington, DC, US. Environmental Protection Agency, EPA Science Advisory Board. 2007. Available: http://yosemite.epa.gov/sab/SABPRODUCT.NSF/81e39f4c09954fcb85256ead006be86e/6f6464d3d773a6ce85257081003b0efe!OpenDocument&TableRow=2.3#2. Accessed on [2014-08-27].

[2] Mississippi River/Gulf of Mexico Watershed Nutrient Task Force. Gulf hypoxia action plan 2008 for reducing, mitigating, and controlling hypoxia in the Northern Gulf of Mexico and improving water quality in the Mississippi River Basin. Washington, DC, US. Environmental Protection Agency, Office of Wetlands, Oceans, and Watersheds, 2008. Available: http://water.epa.gov/type/watersheds/named/msbasin/actionplan.cfm#documents. Accessed on [2014-08-27].

[3] Arnold J G, Srinivasan R, Muttiah R S, Williams J R. Large area hydrologic modeling and assessment part I: model development. J. Amer. Water Resour. Assoc., 1998; 34(1): 73–89. doi: 10.1111/j.1752-1688.1998.tb05961.x.

[4] Williams J R, Arnold J G, Kiniry J R, Gassman P W, Green C W. History of model development at Temple, Texas. Hydrol. Sci. J. 2008; 53(5): 948–960. doi: 10.1623/hysj.53.5.948.

[5] Gassman P W, Reyes M R, Green C H, Arnold J G. The Soil and Water Assessment Tool: historical development, applications, and future research directions. Trans. ASABE. 2007; 50(4): 1211–1250. doi: 10.13031/2013.23634.

[6] Gassman P W, Sadeghi A M, Srinivasan R. Applications of the SWAT model special section: overview and insights. J. Environ. Qual., 2014; 43(1): 1–8. doi: 10.2134/jeq 2013.11.0466.

[7] Douglas-Mankin K R, Srinivasan R, Arnold J G. Soil and Water Assessment Tool (SWAT) model: current developments and applications. Trans. ASABE. 2010; 53(5): 1423–1431. doi: 10.2489/jswc.68.1.41.

[8] Tuppad P, Douglas-Mankin K R, Lee T, Srinivasan R, Arnold J G. Soil and Water Assessment Tool (SWAT) hydrologic/water quality model: extended capability and wider adoption. Trans. ASABE. 2011; 54(5): 1677–1684. doi: 10.13031/2013.34915.

[9] Santhi C, Kannan N, Arnold J G, Di Luzio M. Spatial Calibration and Temporal Validation of Flow for Regional Scale Hydrologic Modeling. J. Amer. Water Resour. Assoc. 2008; 44(4): 829–846. doi: 10.1111/j.1752-1688.2008.00207.x.

[10] Santhi C, Kannan N, White M, Di Luzio M, Arnold J G, Wang X, et al. An integrated modeling approach for estimating the water quality benefits of conservation practices at river basin scale. J. Environ. Qual. 2014; 43(1): 177–198. doi: 10.2134/jeq2011.0460.

[11] USDA-NRCS. Assessment of the Effects of Conservation Practices on Cultivated Cropland in the Ohio-Tennessee River Basin. Washington, D.C.: United States Department of Agriculture, Natural Resources Conservation Service, Conservation Effects Assessment Project. 2011. 173 p. Available http://www.nrcs.usda.gov/wps/portal/nrcs/detail/national/technical/nra/ceap/?cid=stelprdb1046185. Accessed on [2014-08-27].

[12] Panagopoulos Y, Gassman P W, Jha M K, Kling C L,

Campbell T, Srinivasan R, et al. 2014. A refined regional modeling approach for the Corn Belt - experiences and recommendations for large-scale integrated modeling. J. Hydrol. doi: 10.1016/j.jhydrol.2015.02.039.

[13] Kling C L, Panagopoulos Y, Rabotyagov S S, Valcu A M, Gassman P W, Campbell T, et al. LUMINATE: linking agricultural land use, local water quality and Gulf of Mexico hypoxia. Euro.Rev. Agric. Econ. 2014; 41(3): 431–459. doi: 10.1093/erae/jbu009.

[14] White M J, Santhi C, Kannan N, Arnold J G, Harmel D, Norfleet L, et al. Nutrient delivery from the Mississippi River to the Gulf of Mexico and effects of cropland conservation. J. Soil Water Cons. 2014; 69(1): 26–40. doi: 10.2489/jswc. 69.1.26.

[15] Santhi C, Arnold J G, White M, Di Luzio M, Kannan N, Norfleet L, et al. Effects of agricultural conservation practices on N loads in the Mississippi-Atchafalaya River Basin. J. Environ. Qual. 2014; 43(6): 1903–1915. doi: 10.2134/jeq 2013.10.0403.

[16] Rabotyagov S, Campbell T, White M, Arnold J, Atwood A, Norfleet L, et al. Cost-effective targeting of conservation investments to reduce the Northern Gulf of Mexico hypoxic zone. PNAS. 2014; 111(52): 18530–18535. doi: 10.1073/ pnas.1405837111.

[17] Santhi C, White M, Arnold J G, Norfleet L, Atwood J, Kellogg R, et al. Estimating the effects of agricultural conservation practices on phosphorus loads in the Mississippi-Atchafalaya River Basin. Trans. ASABE. 2014; 57(5): 1339–1357. doi: 10.13031/trans.57.10458.

[18] CSCAP. Sustainablecorn.org crops, climate, culture and change: Two-page project summary. Ames, Iowa: Iowa State University, Climate and Corn-based Cropping Systems CAP and Washington, D.C.: U.S. Department of Agriculture, National Institute of Food and Agriculture. 2014. Available: http://www.sustainablecorn.org/About-Project/Index.html. Accessed on [2014-08-27].

[19] USGS. Federal Standards and Procedures for the National Watershed Boundary Dataset (WBD). Techniques and Methods 11-A3, Chapter 3 of Section A, Federal Standards Book 11, Collection and Delineation of Spatial Data, Third edition. Reston, Virginia: U.S. Department of the Interior, U.S. Geological Survey. Washington, D.C.: U.S. Department of Agriculture, Natural Resources Conservation Service. 2012. Available: http://pubs.usgs.gov/tm/tm11a3/. Accessed on [2014-02-13].

[20] USGS. WaterQualityWatch -- Continuous Real-Time Water Quality of Surface Water in the United States. Reston, Virginia: U.S. Department of the Interior, U.S. Geological Survey. 2014. Available: http://waterwatch.usgs.gov/ wqwatch/. Accessed on [2014-01-25].

[21] Arnold J G, Kiniry J R, Srinivasan R, Williams J R, Haney E B, Neitsch S L. Soil and Water Assessment Tool input/output documentation: Version 2012. Technical Report No. 439, Texas Water Resources Institute. 2011. Available: http://swatmodel.tamu.edu/documentation/. Accessed on [2014-08-9].

[22] SWAT. ArcSWAT: ArcGIS-ArcView extension and graphical user input interface for SWAT. Temple, Texas: U.S. Department of Agriculture, Agricultural Research Service, Grassland, Soil & Water Research Laboratory. 2013. Available: http://swat.tamu.edu/software/arcswat/. Accessed on [2013-08-14].

[23] Williams J R, Berndt H D. Sediment yield prediction based on watershed hydrology. Trans. ASAE. 1977; 20(6): 1100–1104. doi: 10.13031/2013.35710.

[24] Arabi M, Frankenberger J R, Engel B A, Arnold J G. Representation of agricultural coservation practices with SWAT. Hydrological Processes, 2008; 22(16): 3042–3055. doi: 10.1002/hyp.6890.

[25] Neitsch S L, Arnold J G, Kiniry J R, Williams J R. Soil and Water Assessment Tool (SWAT) Theoretical Documentation (BRC Report 02-05). Temple, Texas: Texas A&M University System, Texas A&M AgriLife, Blackland Research & Extension Center. 2009. Available: http://swatmodel.tamu. edu/documentation. Accessed on [2014-08-9].

[26] USGS. National elevation dataset. Reston, Virginia: U.S. Department of the Interior, U.S. Geological Survey. 2014. Available: http://ned.usgs.gov/. Accessed on [2014-01-25].

[27] NCDC-NOAA. Climate data online. Asheville, North Carolina: National Oceanic and Atmospheric Administration, National Climatic Data Center, National Climatic Data Center. 2012. Available: http://www.ncdc.noaa.gov/cdo-web/. Accessed on [2014-01-25].

[28] USDA-NASS. Cropland data layer metadata. Washington, D.C., U.S. Department of Agriculture, National Agricultural Statistics Service. 2012. Available: http://www.nass.usda. gov/research/Cropland/metadata/meta.htm. Accessed on [2014-01-25].

[29] USGS. National Land Cover Database (NLCD). Reston, Virginia: U.S. Department of the Interior, U.S. Geological Survey. 2014. Available: http://www.asprs.org/publications/ pers/2007journal/april/highlight.pdf. Accessed on [2014-01-25].

[30] Srinivasan R, Zhang X, Arnold J. SWAT ungauged: hydrological budget and crop yield predictions in the Upper Mississippi River Basin. Trans. ASABE. 2010; 53(5): 1533–1546. doi: 10.13031/2013.34903

[31] USDA-NRCS. Description of STATSGO2 Database. Washington, D.C.: U.S. Department of Agriculture, Natural Resources Conservation Service. 2014. Available:

http://www.nrcs.usda.gov/wps/portal/nrcs/detail/soils/survey/?cid=nrcs142p2_053629. Accessed on [2014-01-25].

[32] Sugg Z. Assessing U.S. Farm Drainage: Can GIS Lead to Better Estimates of Subsurface Drainage Extent?. Washington, D.C.: World Resources Institute. 2007. Available: http://www.wri.org/publication/assessing-u-s-farm-drainage-can-gis-lead-better-estimates-subsurface-drainage-exten. Accessed on [2014-01-25].

[33] Baker N T. Tillage Practices in the Conterminous United States, 1989–2004—Datasets Aggregated by Watershed. Data Series 573. Reston, Virginia: U.S. Department of the Interior, U.S. Geological Survey. 2011. Available: http://pubs.usgs.gov/ds/ds573/. Accessed on [2014-01-25].

[34] Duriancik L F, Bucks D, Dobrowolski J P, Drewes T, Eckles S D, Jolley L, et al. The first five years of the Conservation Effects Assessment Project. J. Soil Water Cons. 2008; 63(6): 185A–197A. doi: 10.2489/jswc.63.6.185A.

[35] Rawls W J, Richardson H H. Runoff curve number for conservation tillage. J. Soil Water Cons, 1983; 38(6): 494–496.

[36] Rawls W J, Onstad C A, Richardson H H. Residue and tillage effects on SCS runoff curve numbers. Trans. ASAE. 1980; 23(2): 357–361. doi: 10.13031/2013.34585.

[37] IPNI. A preliminary Nutrient Use Geographic Information System (NuGIS) for the U.S. Norcross, Georgia: International Plant Nutrition Institute (IPNI). 2010. Available: http://www.ipni.net/nugis. Accessed on [2014-01-25].

[38] Maupin M A, Ivahnenko T. Nutrient loadings to streams of the continental United States from municipal and industrial effluent. J. Amer. Water Resour. Assoc. 2011; 47(5): 950–964. doi: 10.1111/j.1752-1688.2011.00576.x.

[39] Robertson D. Personal communication. Middleton, Wisconsin: U.S. Geological Survey, Wisconsin Water Science Center. 2013. Available: http://wi.water.usgs.gov/professional-pages/robertson.html. Accessed on [2013-10-23].

[40] Abbaspour K C. User Manual for SWAT-CUP 4.3.2. SWAT Calibration and Uncertainty Analysis Programs - A User Manual. Duebendorf, Switzerland: Swiss Federal Institute of Aquatic Science and Technology, Eawag. 2011. 103 p. Available: http://www.neprashtechnology.ca/Default.aspx. Accessed on [2013-10-11].

[41] Abbaspour K C, Yang J, Maximov I, Siber R, Bogner K, Mieleitner, J, et al. Modelling hydrology and water quality in the pre-alpine/alpine Thur watershed using SWAT. J. Hydrol, 2007; 333: 413–430. doi: 10.1016/j.jhydrol.2006.09.014.

[42] Schuol J, Abbaspour K C, Srinivasan R, Yang H. Estimation of freshwater availability in the West African sub-continent using the SWAT hydrologic model. J. Hydrol, 2008; 352(1-2): 30–49. doi: 10.1016/j.jhydrol.2007.12.025.

[43] Schuol J, Abbaspour K C, Yang H, Srinivasan R, Zehnder A J B. Modeling blue and green water availability in Africa. Water Resour. Res. 2008; 44(W07406): 1–18. doi: 10.1029/2007WR006609.

[44] Arnold J G, Moriasi, D N, Gassman, P W, Abbaspour, K C, White, M J, Srinivasan, R, et al. SWAT: model use, calibration, and validation. Trans. ASABE. 2012; 55(4): 1491–1508. doi: 10.13031/2013.42256.

[45] Moriasi D N, Arnold J G, Van Liew M W, Binger R L, Harmel R D, Veith T. Model evaluation guidelines for systematic quantification of accuracy in watershed simulations. Trans. ASABE. 2007; 50(3): 885–900. doi: 10.13031/ 2013.23153.

[46] Krause P, Boyle D P, Bäse F. Comparison of different efficiency criteria for hydrological model assessment. Advances in Geosciences. 2005; 5: 89–97. doi: 10.5194/adgeo-5-89-2005.

[47] LLNL. About the WCRP CMIP3 multi-model dataset archive at PCMDI. Livermore, California: Lawrence Livermore National Laboratory. 2013. Available: http://www-pcmdi.llnl.gov/ipcc/about_ipcc.php. [Accessed 2014-02-15].

[48] Taylor K E, Stouffer R J, Meehl G A. An overview of CMIP5 and the experiment design. Bull. Amer. Meteor. Soc. 2012; 93: 485–498. doi: 10.1175/BAMS-D-11-00094.1.

[49] Panagopoulos, Y, Gassman P W, Arritt R, Herzmann D E, Campbell T, Jha, M K, et al. Surface water quality and cropping systems sustainability under a changing climate in the U.S. Corn Belt region. Journal of Soil Water Conservation, 2014; 69(6): 483–494. doi: 10.2489/jswc.69.6.483.

[50] Knutti R, Sedlacek J. Robustness and uncertainties in the new CMIP5 climate model projections. Nature Clim. Change. 2013; 3: 369–373. doi: 10.1038/nclimate1716.

[51] Frame D J, Booth B B B, Kettleborough J A, Stainforth D A, Gregory J M, Collins M, Allen M R. Constraining climate forecasts: the role of prior assumptions. Geophys. Res. Lett. 2005; 32: L09702. doi: 10.1029/2004GL022241.

[52] Frame D J, Booth B, Kettleborough J A, Stainforth D A, Gregory J M, Collins M, Allen M R. Correction to: "Constraining climate forecasts: the role of prior assumptions", Geophys. Res. Lett. 2014; 41: 3257–3258. doi: 10.1002/ 2014GL059853.

[53] Randall D A, Wood R A, Bony S, Colman R, Fichefet T, Fyfe J, et al. Climate Models and Their Evaluation. In: Solomon S, Qin D, Manning M, Chen Z, Marquis M, Averyt K B, et al. (Eds.). Climate Change 2007: The Physical Science Basis. Contribution of Working Group I to the Fourth Assessment Report of the Intergovernmental Panel on Climate Change. Cambridge, United Kingdom and New

York, New York: Cambridge University Press. 2007.

[54] Meehl G A, Covey C, Delworth T, Latif M, McAvaney B, Mitchell J F B, et al. The WCRP CMIP3 multi-model dataset: A new era in climate change research. Bull. Amer. Meteor. Soc. 2007; 88: 1383–1394. doi: 10.1175/BAMS-88-9-1383.

[55] Kaspar T C, Singer J W. The Use of Cover Crops to Manage Soil. In: Hatfield J L, Sauer T J (Eds). Soil Management: Building a Stable Base for Agriculture. Madison, Wisconsin: American Society of Agronomy and Soil Science Society of America. 2011. pp. 321–337.

[56] Tonitto C, David M B, Drinkwater L E. Replacing bare fallows with cover crops in fertilizer-intensive cropping systems: a meta-analysis of crop yield and N dynamics. Agric. Ecosys. Environ. 2006; 112(1): 58–72. doi: 10.1016/j.agee. 2005.07.003.

[57] Derpsch R, Friedrich T, Kassam A, Hongwen L. Current status of adoption of no-till farming in the world and some of its main benefits. Int J Agric Biol Engr. 2010; 3(1): 1–25. doi: 10.3965/j.issn.1934-6344.2010.01.001-025.

[58] Soane B D, Ball B C, Arvidsson J, Basch G, Moreno F, Roger-Estrade J. No-till in northern, western and south-western Europe: A review of problems and opportunities for crop production and the environment. Soil Till. Res. 2012; 118: 68–87. doi: 10.1016/j.still.2011.10.015.

[59] Ule´ B, Aronsson H, Bechmann M, Krogstad T, Øygarden L, Stenberg M. Soil tillage methods to control phosphorus loss and potential side-effects: A Scandinavian review. Soil Use Manage. 2010; 26(2): 94–107. doi: 10.1111/j.1475-2743. 2010.00266.x.

[60] Krueger E S, Ochsner T E, Porter P M, Baker J M. Winter Rye Cover Crop Management Influences on Soil Water, Soil Nitrate, and Corn Development. Agron. J. 2011; 103(2): 316–323. doi: 10.2134/agronj2010.0327.

[61] Singer J, Kaspar T, Pedersen P. Small grain cover crops for corn and soybean. PM 1999. Ames, Iowa: Iowa State University Extension. 2005. Available: https://store.extension.iastate.edu/Product/Small-Grain-Cover-Crops-for-Corn-and-Soybean. Accessed on [2014-08-29].

[62] IDALS. Iowa Nutrient Reduction Strategy: a science and technology-based framework to assess and reduce nutrients to Iowa waters and the Gulf of Mexico. Des Moines, Iowa: Iowa Department of Agriculture and Land Stewardship (IDALS); Des Moines, Iowa: Iowa Department of Natural Resources (IDNR); and Ames, Iowa: Iowa State University College of Agriculture and Life Sciences (ISUCALS). 2013. Available http://www.nutrientstrategy.iastate.edu/documents. Accessed on [2013-10-11].